Synthesis and Structural and Magnetic Properties of Mononuclear, Dinuclear, and Tetranuclear Copper(II) Complexes of a 17-Membered Macrocyclic Ligand (HM3), Capable of Forming Endogenous Phenoxide and Pyridazino Bridges. X-ray Crystal Structures of $[Cu_2(M3)(\mu_2\text{-}OMe)(NO_3)_2]$, $[Cu_4(M3)_2(\mu_3\text{-}OMe)_2(\mu_2\text{-}Cl)_2Cl_2]$, $[Cu_4(M3)_2(\mu_3\text{-}OEt)_2(\mu_2\text{-}N_3)_2(N_3)_2](MeOH)$, $[Cu_4(M3)_2(\mu_3\text{-}OMe)_2(NCS)_4](DMF)$, and $[Cu(M3)(NCS)_2]$

Santokh S. Tandon, Laurence K. Thompson,* John N. Bridson, and Monica Bubenik

Department of Chemistry, Memorial University of Newfoundland, St. John's, Newfoundland, Canada A1B 3X7

Received February 10, 1993•

A series of copper(II) complexes, involving dinuclear, tetranuclear, and mononuclear derivatives, $[Cu_2(M3)(\mu_2\text{-}OMe)X_2]$ (X = NO_3 (I), CF_3SO_3 (II)), $[Cu_4(M3)_2(\mu_3\text{-}OMe)_2(\mu_2\text{-}Cl)_2Cl_2]$ (III), $[Cu_4(M3)_2(\mu_3\text{-}OEt)_2(\mu_2\text{-}N_3)_2(N_3)_2](MeOH)$ (IV), $[Cu_4(M3)_2(\mu_3\text{-}OMe)_2(NCS)_4](DMF)$ (V), $[Cu_4(M3)_2(\mu_3\text{-}OMe)_2(\mu_2\text{-}Br)_2Br_2]\cdot 2H_2O$ (VI), and $[Cu(M3)(NCS)_2]$ (VII), have been synthesized by template condensation of 2,6-diformyl-4-methylphenol with 3,6-bis(2-aminoethyl)thio)pyridazine (1:1), in the presence of copper(II) salts, followed, in some cases, by addition of potentially coordinating anions. The tetranuclear complexes III–VI involve an effective dimerization of two dinuclear halves, with an unusual combination of μ_3-alkoxy and μ_2-anion bridges in III, IV, and VI and just μ_3-alkoxy bridges in V. Single-crystal X-ray structures for I, III–V, and VII have been determined. I crystallized in the monoclinic system, space group $P2_1/n$, with a = 8.6930(8) Å, b = 15.02(1) Å, c = 18.308(2) Å, β = 90.890(7)°, and Z = 4. Refinement by full-matrix least-squares procedures gave final residuals of R = 0.057 and R_w = 0.049. III crystallized in the monoclinic system, space group $P2_1/n$, with a = 11.045(2) Å, b = 16.054(6) Å, c = 12.309(2) Å, β = 90.68(2)°, and Z = 4. Refinement by full-matrix least-squares procedures gave final residuals of R = 0.032 and R_w = 0.032. IV crystallized in the monoclinic system, space group $P2_1/n$, with a = 11.077(3) Å, b = 15.153(4) Å, c = 16.492(2) Å, β = 99.45(2)°, and Z = 4. Refinement by full-matrix least-squares procedures gave final residuals of R = 0.059 and R_w = 0.049. V crystallized in the monoclinic system, space group $C2/c$, with a = 27.316(5) Å, b = 22.170(4) Å, c = 11.036(4) Å, β = 111.81(2)°, and Z = 8. Refinement by full-matrix least-squares procedures gave final residuals of R = 0.056 and R_w = 0.061. VII crystallized in the monoclinic system, space group $P2/n$, with a = 21.283(6) Å, b = 11.367(6) Å, c = 21.679(4) Å, β = 116.73(1)°, and Z = 8. Refinement by full-matrix least-squares procedures gave final residuals of R = 0.042 and R_w = 0.035. Low magnetic moments are observed for all the polynuclear complexes, signifying the presence of intradimer antiferromagnetic coupling. This has been confirmed by variable-temperature magnetic studies, and strong exchange is observed within each dinuclear fragment (I–VI), with $-2J > 445$ cm^{-1} in all cases. Weak interdinuclear ferromagnetic exchange is apparent in two cases, but for complex IV, in which bridging azides link the dinuclear halves, much stronger antiferromagnetic interdimer coupling appears to exist.

Introduction

Macrocyclic ligands derived by template condensation of 2,6-diformyl-4-R-phenol and 2,6-diacetyl-4-R-phenol (R = Me, tBu) with simple diamines (e.g. 1,2-ethanediamine, 1,3-propanediamine, 1,4-butanediamine, etc.) generally produce 2:2 macrocyclic rings, encompassing two metals, bridged by two phenoxide groups and each bound terminally by two imine nitrogen donors. Such complexes, particularly in the case of copper, are strongly antiferromagnetically coupled and exhibit well-defined one-electron redox processes.[1-20] The incorporation of longer diamine fragments, with additional donor groups, e.g. 2-hydroxy-1,3-diaminopropane, 3-hydroxy-1,5-diaminopentane, and 2,6-bis(aminomethyl)-4-methylphenol, increases the coordination capacity of the resulting macrocycles, and four and even six metals can be accommodated within the same macrocyclic ring.[21-27] The

* Author to whom correspondence should be addressed.

• Abstract published in *Advance ACS Abstracts*, September 15, 1993.

(1) Pilkington, N. H.; Robson, R. *Aust. J. Chem.* **1970**, *23*, 2225.
(2) Okawa, H.; Kida, S. *Bull. Chem. Soc. Jpn.* **1972**, *45*, 1759.
(3) Addison, A. W. *Inorg. Nucl. Chem. Lett.* **1976**, *12*, 899.
(4) Hoskins, B. F.; McLeod, N. J.; Schaap, H. A. *Aust. J. Chem.* **1976**, *29*, 515.
(5) Gagné, R. R.; Koval, C. A.; Smith, T. J. *J. Am. Chem. Soc.* **1977**, *99*, 8367.
(6) Lambert, S. L.; Hendrickson, D. N. *Inorg. Chem.* **1979**, *18*, 2683.
(7) Gagné, R. R.; Koval, C. A.; Smith, T. J.; Cimolino, M. C. *J. Am. Chem. Soc.* **1979**, *101*, 4571.
(8) Gagné, R. R.; Henling, L. M.; Kistenmacher, T. J. *Inorg. Chem.* **1980**, *19*, 1226.
(9) Mandal, S. K.; Nag, K. *J. Chem. Soc., Dalton Trans.* **1983**, 2429.
(10) Long, R. S.; Hendrickson, D. N. *J. Am. Chem. Soc.* **1983**, *105*, 1513.
(11) Mandal, S. K.; Nag, K. *J. Chem. Soc., Dalton Trans.* **1984**, 2141.
(12) Carlisle, W. D.; Fenton, D. E.; Roberts, P. B.; Casellato, U.; Vigato, P. A.; Graziani, R. *Transition Met. Chem. (London)* **1986**, *11*, 292.
(13) Mandal, S. K.; Thompson, L. K.; Nag, K.; Charland, J.-P.; Gabe, E. J. *Inorg. Chem.* **1987**, *26*, 1391.
(14) Mandal, S. K.; Thompson, L. K.; Nag, K.; Charland, J.-P.; Gabe, E. J. *Can. J. Chem.* **1987**, *65*, 2815.
(15) Mandal, S. K.; Thompson, L. K.; Nag, K.; *Inorg. Chim. Acta* **1988**, *149*, 247.
(16) Lacroix, P.; Kahn, O.; Gleizes, A.; Valade, L.; Cassoux, P. *Nouv. J. Chim.* **1984**, *8*, 643.
(17) Lacroix, P.; Kahn, O.; Theobald, F.; Leroy, J.; Wakselman, C. *Inorg. Chim. Acta* **1988**, *142*, 129.
(18) Mandal, S. K.; Thompson, L. K.; Newlands, M. J.; Gabe, E. J. *Inorg. Chem.* **1989**, *28*, 3707.
(19) Hendrickson, D. N.; Long, R. C.; Hwang, Y. T.; Chang, H.-R. In *Biological and Inorganic Copper Chemistry*; Eds. Karlin, K. D., Zubieta, J., Eds.; Adenine Press: Guilderland, NY, 1985; p 223.
(20) Mandal, S. K.; Thompson, L. K.; Newlands, M. J.; Gabe, E. J. *Inorg. Chem.* **1990**, *29*, 1324.
(21) McKee, V.; Tandon, S. S. *J. Chem. Soc., Chem. Commun.* **1988**, 385.

0020-1669/93/1332-4621$04.00/0 © 1993 American Chemical Society

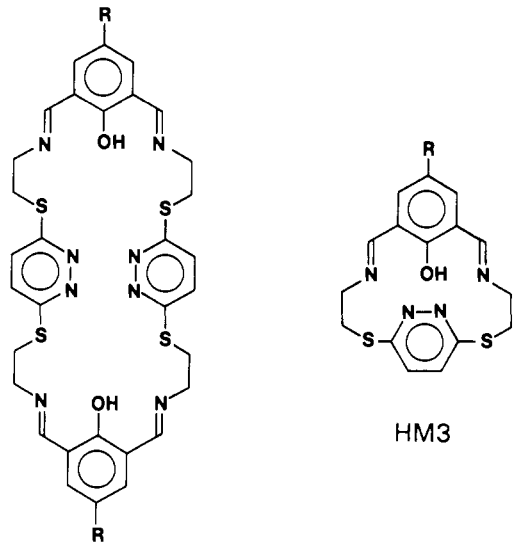

H_2M1, R = CH_3
H_2M2, R = $C(CH_3)_3$

Figure 1. Macrocyclic ligands.

template condensation of 2,6-diformyl-4-R-phenol (R = Me, tBu), with 3,6-bis((2-aminoethyl)thio)pyridazine (PTA) in the presence of copper perchlorate and tetrafluoroborate led to the formation of the 34-membered (2:2) macrocyclic ligands H_2M1 and H_2M2 (Figure 1), in which the pyridazine fragments were considered as dinucleating centers in their own right.[28-35] However, with these copper salts, involving weakly coordinating or noncoordinating anions (e.g. BF_4 and ClO_4), dinuclear derivatives were obtained, in which the two distorted copper(II) centers are bound in the familiar diphenoxide-bridged structure, with terminal, in-plane imine donors. In organizing the two phenoxide fragments about the dinuclear center, the ligand adopts a most unusual twist, in which the pyridazine fragments loop over the copper atoms and are involved in weak axial coordination.[36]

In the present study, the template condensation of 2,6-diformyl-4-methylphenol with PTA in the presence of copper(II) nitrate and trifluoromethanesulfonate (triflate) leads to the formation of dinuclear copper(II) complexes of the 17-membered (1:1) macrocyclic ligand HM3 (Figure 1), with two oxygen bridges (phenoxide and methoxide) between the copper centers. Treatment of $[Cu_2(M3)(\mu_2\text{-}OMe)(NO_3)_2]$ (**I**) with chloride, azide, thiocyanate, and bromide produces the tetranuclear derivatives $[Cu_4(M3)_2(\mu_3\text{-}OMe)_2(\mu_2\text{-}Cl)_2Cl_2]$ (**III**), $[Cu_4(M3)_2(\mu_3\text{-}OEt)_2(\mu_2\text{-}N_3)_2(N_3)_2](MeOH)$ (**IV**), $[Cu_4(M3)_2(\mu_3\text{-}OMe)_2(NCS)_4]$·(DMF) (**V**), and $[Cu_4(M3)_2(\mu_3\text{-}OMe)_2(\mu_2\text{-}Br)_2Br_2]\cdot 2H_2O$ (**VI**), respectively. The pyridazine rings appear not to be involved in coordination in these complexes. Low room-temperature magnetic moments (0.38–1.02 μ_B) in all these polynuclear species signify the presence of antiferromagnetic coupling, which is confirmed by variable-temperature magnetic measurements.

Experimental Section

Synthesis of Complexes. (a) $[Cu_2(M3)(\mu_2\text{-}OMe)(NO_3)_2]$ (I), $[Cu_2(M3)(\mu_2\text{-}OMe)(CF_3SO_3)_2]\cdot 2C_2H_5OH$ (II), and $[Cu(M3)(NCS)_2]$ (VII). 2,6-Diformyl-4-methylphenol[37] (0.164 g, 1.00 mmol), dissolved in 50 mL of hot methanol, was added to a solution of $Cu(NO_3)_2\cdot 3H_2O$ (0.438 g, 2.00 mmol) in 50 mL of methanol. The resulting green solution was refluxed for 15 min, and a solution of 3,6-bis((2-aminoethyl)thio)pyridazine (PTA)[36] (0.230 g, 1.00 mmol) in 100 mL of methanol was added dropwise over a period of 15 min. The resulting mixture was refluxed for 20 h. A bright green solid formed, which was filtered off, washed with methanol (3 × 5 mL), and dried under vacuum. Recrystallization by diffusion of ether into a DMF/MeOH solution of the complex produced blue-green crystals suitable for X-ray analysis (yield: 31%). Anal. Calcd for $[Cu_2(C_{17}H_{17}N_4OS_2)(OCH_3)(NO_3)_2]$: C, 33.80; H, 3.13; N, 13.15; Cu, 19.87. Found: C, 34.09; H, 3.30; N, 13.13; Cu, 19.65. **II** was prepared in a similar manner using copper triflate. However the final reaction mixture in methanol was reduced to a volume of about 20 mL and ethanol (50 mL) added. On standing, a light green powder formed, which was filtered off, washed with ethanol, and dried under vacuum (yield: 75%). Anal. Calcd for $[Cu_2(C_{17}H_{17}N_4OS_2)(OCH_3)(CF_3SO_3)_2]\cdot 2C_2H_5OH$: C, 31.82; H, 3.54; N, 6.19; Cu, 14.03. Found: C, 31.65; H, 2.90; N, 5.96; Cu, 13.75. **VII** was prepared in a similar manner by reacting 2,6-diformyl-4-methylphenol with PTA and 2 equiv of $Cu(NCS)_2$ (generated from the reaction of $Cu(NO_3)_2$ and KSCN in methanol followed by filtration to remove KNO_3) in methanol. However during the course of the reaction a brown insoluble solid formed (copper(I) thiocyanate), which was filtered off, and the mother liquor was concentrated to give green crystals as the major component. A small amount of a bluish-green crystalline material was also obtained, which was shown to be structurally identical to the tetranuclear thiocyanate complex **V**.

(b) $[Cu_4(M3)_2(\mu_3\text{-}OMe)_2(\mu_2\text{-}Cl)_2Cl_2]$ (III), $[Cu_4(M3)_2(\mu_3\text{-}OEt)_2(\mu_2\text{-}N_3)_2(N_3)_2](MeOH)$ (IV), $[Cu_4(M3)_2(\mu_3\text{-}OMe)_2(NCS)_4](DMF)$ (V), $[Cu_4(M3)_2(\mu_3\text{-}OMe)_2(\mu_2\text{-}Br)_2Br_2]\cdot 2H_2O$ (VI). **III** was obtained as green crystals, suitable for X-ray analysis, by adding a mixture of $NH_4Cl/CuCl_2$ (excess) dissolved in DMF/MeOH (1:1) to a solution of **I** in DMF/MeOH. **VI** was prepared in a similar manner by reaction of **I** with a mixture of $NH_4Br/CuBr_2$ in DMF/MeOH. **IV** was prepared similarly by treating **I** with sodium azide in a mixture of MeOH/EtOH/DMF to give dark green crystals suitable for X-ray analysis. **V** was prepared similarly by adding a methanolic solution of NH_4NCS to a solution of **I** in DMF/MeOH and was obtained as blue-green crystals suitable for X-ray analysis. Anal. Calcd for $[Cu_4(C_{17}H_{17}N_4OS_2)_2(OCH_3)_2Cl_4]\cdot 2H_2O$: C, 36.61; H, 4.10; N, 9.49; Cu, 21.52. Found: C, 36.99; H, 3.60; N, 9.25; Cu, 20.97. Anal. Calcd for $[Cu_4(C_{17}H_{17}N_4OS_2)(OCH_3)_2(NCS)_4](DMF)$ (dried sample): C, 38.53; H, 3.53; N, 13.59. Found: C, 38.49; H, 3.47; N, 13.89. Anal. Calcd for $[Cu_4(C_{17}H_{17}N_4OS_2)_2(OCH_3)_2Br_4]\cdot 2H_2O$: C, 31.18; H, 3.19; N, 8.08. Found: C, 31.09; H, 2.79; N, 8.40.

Physical Measurements. Infrared spectra were recorded as Nujol mulls using a Mattson Polaris FT-IR instrument. Electronic spectra were recorded as mulls using Cary 17 and Cary 5E spectrometers. Room-temperature magnetic moments were measured using a Cahn 7600 Faraday magnetic balance, and variable-temperature magnetic data (4–300 K) were obtained using an Oxford Instruments superconducting Faraday susceptometer with a Sartorius 4432 microbalance. A main solenoid field of 1.5 T and a gradient field of 10 T m^{-1} were employed.

C, H, and N analyses were carried out by Canadian Microanalytical Service, Delta, Canada, and copper was analyzed by EDTA titration.

Safety Note! Azide compounds are potentially explosive and should be treated with care and in small quantities. In particular copper(II) azide is explosive, and reactions involving the mixing of an excess of a copper(II) salt and ligand, followed by addition of excess azide, should be avoided. A small explosion resulted when a small quantity of the azide complex was synthesized in this way, which was attributed to copper azide impurity. Metathesis from the corresponding nitrate complex did not produce explosive material.

(22) McKee, V.; Tandon, S. S. *J. Chem. Soc., Chem. Commun.* **1988**, 1334.
(23) McKee, V.; Tandon, S. S. *Inorg. Chem.* **1989**, *28*, 2901.
(24) Tandon, S. S.; Mckee, V. *J. Chem. Soc., Dalton Trans.* **1991**, 221.
(25) Tandon, S. S.; Mckee, V. Unpublished results.
(26) Tandon, S. S.; Thompson, L. K.; Bridson, J. N. *J. Chem. Soc., Chem. Commun.* **1992**, 911.
(27) Hoskins, B. F.; Robson, R.; Smith, P. *J. Chem. Soc., Chem. Commun.* **1990**, 488.
(28) Mandal, S. K.; Thompson, L. K.; Gabe, E. J.; Charland, J.-P.; Lee, F. L. *Inorg. Chem.* **1988**, *27*, 855.
(29) Thompson, L. K.; Mandal, S. K.; Charland, J.-P.; Gabe, E. J. *Can. J. Chem.* **1988**, *66*, 348.
(30) Thompson, L. K.; Mandal, S. K.; Rosenberg, L.; Lee, F. L.; Gabe, E. J. *Inorg. Chim. Acta* **1987**, *133*, 81.
(31) Mandal, S. K.; Thompson, L. K.; Gabe, E. J.; Lee, F. L.; Charland, J.-P. *Inorg. Chem.* **1987**, *26*, 2384.
(32) Woon, T. C.; McDonald, R.; Mandal, S. K.; Thompson, L. K.; Connors, S. P.; Addison, A. W. *J. Chem. Soc., Dalton Trans.* **1986**, 2381.
(33) Mandal, S. K.; Thompson, L. K.; Newlands, M. J.; Lee, F. L.; LePage, Y.; Charland, J.-P.; Gabe, E. J. *Inorg. Chim. Acta* **1986**, *122*, 199.
(34) Thompson, L. K.; Lee, F. L.; Gabe, E. J. *Inorg. Chem.* **1988**, *27*, 39.
(35) Thompson, L. K.; Mandal, S. K.; Gabe, E. J.; Lee, F. L.; Addison, A. W. *Inorg. Chem.* **1987**, *26*, 657.
(36) Tandon, S. S.; Thompson, L. K.; Bridson, J. N. *Inorg. Chem.* **1993**, *32*, 32.
(37) Ullman, F.; Brittner, K. *Chem. Ber.* **1909**, *42*, 2539.

Table I. Summary of Crystallographic Data for I, III–V, and VII

	I	III	IV	V	VII
empirical formula	$Cu_2S_2O_8N_6C_{18}H_{20}$	$Cu_2S_2O_2N_4C_{18}H_{20}$	$Cu_2S_2O_3N_{10}C_{20}H_{26}$	$Cu_2S_4O_3N_{6.5}C_{26.1}H_{20}$	$CuS_4ON_6C_{19}H_{20}$
fw	639.6	586.5	645.7	728.02	538.18
cryst syst	monoclinic	monoclinic	monoclinic	monoclinic	monoclinic
space group	$P2_1/n$	$P2_1/n$	$P2_1/n$	$C2/c$	$P2/n$
a (Å)	8.6930(8)	11.045(2)	11.077(3)	27.316(5)	21.283(6)
b (Å)	15.02(1)	16.054(6)	15.153(4)	22.170(4)	11.367(6)
c (Å)	18.308(2)	12.309(2)	16.492(2)	11.036(4)	21.679(4)
β (deg)	90.890(7)	90.68(2)	99.45(2)	111.81(2)	116.73(1)
V (Å)^3	2391(2)	2182(1)	2731(1)	6205(3)	4684(3)
Z	4	4	4	8	8
ρ(calcd) (g cm^{-3})	1.777	1.785	1.571	1.559	1.526
μ (cm^{-1})	20.07	24.09	17.49	16.71	13.00
radiation, λ (Å)	Mo Kα, 0.710 69	Mo Kα, 0.710 69	Mo Kα, 0.710 69	Mo Kα, 0.710 69	Mo Kα, 0.710 69
T (°C)	26(1)	25(1)	25(1)	−114(1)	25(1)
$2\theta_{max}$ (deg)	50.0	50.0	50.0	50.0	50.0
no. of obsd reflns	4705	4206	5266	5742	8951
no. of unique reflns	27725 ($I > 3.0\sigma(I)$)	2891 ($I > 3.0\sigma(I)$)	1805 ($I > 3.0\sigma(I)$)	4056 ($I > 2.0\sigma(I)$)	4579 ($I > 3.0\sigma(I)$)
GOF	2.77	1.44	1.89	3.02	1.61
R^a	0.057	0.032	0.059	0.056	0.042
$R_w{}^b$	0.049	0.032	0.049	0.061	0.035

^{a} $R = \sum(|F_o| - |F_c|)/\sum(|F_c|)$. ^{b} $R_w = [(\sum w(|F_o| - |F_c|)^2/\sum w(|F_o|)^2]^{1/2}$.

Table II. Final Atomic Positional Parameters and B_{eq} Values (Å^2) for $[Cu_2(M3)(\mu_2\text{-OMe})(NO_3)_2]$ (I)

atom	x	y	z	$B_{eq}{}^a$	atom	x	y	z	$B_{eq}{}^a$
Cu(1)	0.5141(1)	0.11801(8)	0.65481(6)	3.09(5)	C(1)	0.2571(9)	0.0229(5)	0.7262(5)	2.3(4)
Cu(2)	0.5142(1)	0.09826(8)	0.81443(6)	3.29(5)	C(2)	0.1824(9)	0.0100(5)	0.6576(5)	2.2(4)
S(1)	0.2027(3)	0.3011(2)	0.5735(1)	4.0(1)	C(3)	0.046(1)	−0.0385(6)	0.6542(5)	3.2(5)
S(2)	0.1947(3)	0.2642(2)	0.9086(1)	4.4(1)	C(4)	−0.025(1)	−0.0718(6)	0.7165(5)	3.2(5)
O(1)	0.3968(6)	0.0553(4)	0.7297(3)	2.7(3)	C(5)	0.038(1)	−0.0478(5)	0.7830(5)	2.9(4)
O(2)	0.6448(6)	0.1311(4)	0.7376(3)	4.0(3)	C(6)	0.1775(9)	−0.0009(5)	0.7895(5)	2.3(4)
O(3)	0.6763(6)	0.1597(4)	0.5861(3)	3.8(3)	C(7)	−0.170(1)	−0.1249(7)	0.7112(6)	5.0(6)
O(4)	0.6964(8)	0.0165(4)	0.5824(4)	4.7(4)	C(8)	0.229(1)	0.0563(6)	0.5908(4)	2.5(4)
O(5)	0.8699(7)	0.0986(5)	0.5321(4)	5.4(4)	C(9)	0.364(1)	0.1545(6)	0.5166(5)	3.4(5)
O(6)	0.6742(7)	0.1200(5)	0.8928(3)	4.1(3)	C(10)	0.375(1)	0.2533(6)	0.5352(5)	3.4(5)
O(7)	0.6904(8)	−0.0221(5)	0.8725(4)	5.2(4)	C(11)	0.213(1)	0.2851(5)	0.6686(5)	2.8(4)
O(8)	0.8567(7)	0.0431(5)	0.9445(4)	5.5(4)	C(12)	0.088(1)	0.3228(6)	0.7060(5)	3.4(5)
N(1)	0.3501(7)	0.1022(5)	0.5830(4)	2.6(3)	C(13)	0.088(1)	0.3149(6)	0.7791(5)	3.7(5)
N(2)	0.3286(7)	0.2457(5)	0.7021(4)	2.6(3)	C(14)	0.2107(9)	0.2706(6)	0.8136(5)	3.1(5)
N(3)	0.3269(7)	0.2362(4)	0.7777(4)	2.5(3)	C(15)	0.368(1)	0.2144(7)	0.9442(5)	4.2(5)
N(4)	0.3456(7)	0.0717(5)	0.8801(4)	2.8(4)	C(16)	0.357(1)	0.1131(8)	0.9525(5)	4.1(5)
N(5)	0.7503(8)	0.0901(6)	0.5661(4)	3.7(4)	C(17)	0.224(1)	0.0304(6)	0.8624(5)	2.8(4)
N(6)	0.7431(9)	0.0454(7)	0.9029(4)	4.1(5)	C(18)	0.801(1)	0.1530(7)	0.7399(6)	5.2(6)

^{a} $B_{eq} = (8\pi^2/3)\sum_{i=1}^{3}\sum_{j=1}^{3}U_{ij}a_i^*a_j^*\bar{a}_i\bar{a}_j$.

Crystallographic Data Collection and Refinement of the Structures. (a) $[Cu_2(M3)(\mu_2\text{-OMe})(NO_3)_2]$ (I). Crystals of I are blue-green. The diffraction intensities of an approximately 0.40 × 0.30 × 0.20 mm crystal were collected with graphite-monochromatized Mo Kα radiation and a Rigaku AFC6S diffractometer using the ω–2θ scan mode to $2\theta_{max}$ = 50.0°. A total of 4705 reflections were measured, of which 4475 were unique (R_{int} = 0.084) and 2772 were considered significant with $I_{net} > 3.0\sigma(I_{net})$. An empirical absorption correction was applied, using the program DIFABS,[38] which resulted in transmission factors ranging from 0.80 to 1.28. The data were corrected for Lorentz and polarization effects. The cell parameters were obtained from a least-squares refinement of the setting angles of 25 carefully centered reflections in the range 21.25° < 2θ <29.36°.

The structure was solved by direct methods,[39,40] and the non-hydrogen atoms were refined anisotropically. The final cycle of full-matrix least-squares refinement was based on 2772 reflections and 154 variable parameters and converged with R = 0.057 and R_w = 0.049, with weights based on counting statistics. The maximum and minimum peaks on the final difference map corresponded to 0.66 and −0.70 e/Å^3, respectively. Neutral-atom scattering factors[41] and anomalous dispersion terms[42,43] were taken from the usual sources. All calculations were performed with the TEXSAN[44] crystallographic software package using a VAX 3100 work station. A summary of crystal and other data is given in Table I, and atomic coordinates are given in Table II. Hydrogen atom coordinates (Table SI) and thermal parameters (Table SII) are included as supplementary material.

(b) III–V and VII. Diffraction data collection and structural refinement were carried out in a similar manner for these compounds. In IV a disordered methanol molecule appears to oscillate between two principal positions in the lattice, pivoting on the methyl group, and has been modeled with two oxygen positions O(3) and O(4) (0.35 and 0.65 occupancy, respectively). A single hydrogen-bonding contact from H(1) (bound to O(4)) to terminal azide nitrogen N(10) (2.535 Å) may explain the odd anisotropy of this atom. The crystallographic sample of V contained lattice solvent, which could not be unequivocally assigned. A disordered DMF molecule (assigned O(3), C(21), N(7), C(22), C(23), C(24), C(25)), a disordered methanol (C(32), O(5)), and a less well defined solvent site (C(26)–C(31)) could not be successfully interpreted (positional parameters for these atoms are included in supplementary Table SVII). Crystallographic data were calculated on the basis of the empirical formula $Cu_2S_4O_3N_{6.5}C_{26.1}H_{20}$. The crystals of this complex were found to be unstable and lost solvent of crystallization readily. They were kept under their mother liquor prior to analysis, and the structural determination was done at low temperature. The apparent nonstoichiometric and disordered nature of the lattice solvent was clearly a result of this instability. Solvent hydrogens and that on O(2) were not located. However the main

(38) Walker, N.; Stuart, D. *Acta Crystallogr.* **1983**, *A39*, 158.
(39) Gilmore, C. J. *J. Appl. Crystallogr.* **1984**, *17*, 42.
(40) Beurskens, P. T. DIRDIF: Technical Report 1984/1; Crystallography Laboratory: Toernooiveld, 6525 Ed Nijmegen, The Netherlands, 1984.
(41) Cromer, D. T.; Waber, J. T. *International Tables for X-ray Crystallography*; The Kynoch Press: Birmingham, U.K., 1974; Vol. IV, Table 2.2A.
(42) Ibers, J. A.; Hamilton, W. C. *Acta Crystallogr.* **1974**, *17*, 781.
(43) Cromer, D. T. *International Tables for X-ray Crystallography*; The Kynoch Press: Birmingham, U.K., 1974; Vol. IV, Table 2.3.1.
(44) *Texsan-Texray Structure Analysis Package*; Molecular Structure Corp.: The Woodlands, TX, 1985.

Table III. Final Atomic Positional Parameters and B_{eq} Values (Å²) for $[Cu_4(M3)_2(\mu_3\text{-}OMe)_2(\mu_2\text{-}Cl)_2Cl_2]$ (III)

atom	x	y	z	B_{eq}[a]	atom	x	y	z	B_{eq}[a]
Cu(1)	–0.02989(4)	0.40107(3)	0.46018(4)	2.18(2)	C(4)	0.0704(4)	0.4121(2)	0.2104(3)	2.3(2)
Cu(2)	0.23518(4)	0.43287(3)	0.52450(4)	2.16(2)	C(5)	0.0990(4)	0.4366(3)	0.1045(3)	2.8(2)
Cl(1)	–0.20556(9)	0.40716(7)	0.55253(8)	2.60(4)	C(6)	0.2125(4)	0.4653(3)	0.0765(3)	2.8(2)
Cl(2)	0.3322(1)	0.46319(8)	0.68136(8)	3.22(5)	C(7)	0.3022(4)	0.4606(3)	0.1561(3)	2.8(2)
S(1)	–0.0921(1)	0.20181(9)	0.4742(1)	4.51(7)	C(8)	0.2795(4)	0.4364(3)	0.2631(3)	2.3(2)
S(2)	0.4616(1)	0.22598(8)	0.4097(1)	3.81(6)	C(9)	0.1591(3)	0.4165(2)	0.2933(3)	2.0(2)
O(1)	0.1334(2)	0.3992(2)	0.3960(2)	2.1(1)	C(10)	0.3827(4)	0.4243(3)	0.3344(3)	2.6(2)
O(2)	0.0718(2)	0.4355(2)	0.5089(2)	2.5(1)	C(11)	0.4979(4)	0.3876(3)	0.4878(3)	2.7(2)
N(1)	–0.0955(3)	0.3582(2)	0.3204(3)	2.5(2)	C(12)	0.4966(4)	0.2971(3)	0.5204(4)	3.1(2)
N(2)	0.3813(3)	0.4122(2)	0.4379(3)	2.2(1)	C(13)	0.3020(4)	0.2167(3)	0.4187(4)	3.0(2)
N(3)	0.2524(4)	0.2309(3)	0.5145(3)	3.8(2)	C(14)	0.2343(5)	0.1923(3)	0.3283(4)	3.8(2)
N(4)	0.1307(4)	0.2265(3)	0.5243(3)	3.9(2)	C(15)	0.1122(5)	0.1850(3)	0.3387(4)	3.8(2)
C(1)	–0.1761(4)	0.2173(4)	0.3480(4)	4.4(3)	C(16)	0.0632(4)	0.2053(3)	0.4397(4)	3.3(2)
C(2)	–0.2051(4)	0.3074(3)	0.3193(4)	3.2(2)	C(17)	0.2399(5)	0.4962(3)	–0.0371(4)	4.0(2)
C(3)	–0.0474(4)	0.3756(3)	0.2283(3)	2.6(2)	C(18)	0.0495(4)	0.4023(3)	0.6869(3)	3.2(2)

[a] $B_{eq} = (8\pi^2/3)\sum_{i=1}^{3}\sum_{j=1}^{3}U_{ij}a_i^*a_j^*\bar{a}_i\bar{a}_j$.

Table IV. Final Atomic Positional Parameters and B_{eq} Values (Å²) for $[Cu_4(M3)_2(\mu_3\text{-}OC_2H_5)_2(\mu_2\text{-}N_3)_2(N_3)_2](MeOH)$ (IV)

atom	x	y	z	B_{eq}[a]	atom	x	y	z	B_{eq}[a]
Cu(1)	0.2740(1)	0.4403(1)	0.5153(1)	3.51(9)	C(2)	0.151(1)	0.4289(9)	0.3181(9)	3.4(7)
Cu(2)	0.5137(1)	0.4055(1)	0.4539(1)	2.97(8)	C(3)	0.092(1)	0.431(1)	0.237(1)	4.5(8)
S(1)	0.5124(6)	0.1548(3)	0.3182(3)	5.3(2)	C(4)	0.152(2)	0.425(1)	0.171(1)	5.1(9)
S(2)	0.0253(4)	0.2120(3)	0.4468(4)	6.8(3)	C(5)	0.277(2)	0.409(1)	0.189(1)	5.2(8)
O(1)	0.3391(7)	0.4212(6)	0.4131(5)	3.5(5)	C(6)	0.343(1)	0.405(1)	0.2692(8)	3.5(7)
O(2)	0.4492(7)	0.4358(5)	0.5508(5)	2.9(4)	C(7)	0.090(2)	0.433(1)	0.081(1)	8(1)
O(3)	0.243(9)	0.068(6)	0.665(6)	22(7)	C(8(	0.468(1)	0.3717(9)	0.279(1)	4.2(8)
O(4)	0.082(3)	0.019(2)	0.617(2)	17(2)	C(9)	0.649(1)	0.3100(9)	0.3430(8)	3.7(7)
N(1)	0.544(1)	0.3643(7)	0.3484(8)	3.9(6)	C(10)	0.629(1)	0.221(1)	0.380(1)	4.5(8)
N(2)	0.376(1)	0.2204(8)	0.4264(8)	4.3(7)	C(11)	0.381(1)	0.177(1)	0.360(1)	4.2(8)
N(3)	0.271(1)	0.2323(8)	0.4550(8)	4.9(7)	C(12)	0.274(2)	0.143(1)	0.311(1)	6(1)
N(4)	0.107(1)	0.4155(7)	0.4580(8)	3.6(6)	C(13)	0.168(2)	0.154(1)	0.341(1)	6(1)
N(5)	0.686(1)	0.4023(8)	0.5069(7)	3.7(6)	C(14)	0.166(2)	0.200(1)	0.414(1)	5(1)
N(6)	0.734(1)	0.3479(9)	0.5537(8)	4.2(7)	C(15)	0.050(1)	0.286(1)	0.532(1)	6(1)
N(7)	0.787(1)	0.298(1)	0.600(1)	10(1)	C(16)	0.017(1)	0.385(1)	0.509(1)	6(1)
N(8)	0.221(2)	0.465(1)	0.613(1)	7(1)	C(17)	0.075(1)	0.419(1)	0.379(1)	4.3(8)
N(9)	0.237(1)	0.429(1)	0.671(1)	8(1)	C(18)	0.499(1)	0.398(1)	0.6316(8)	3.7(7)
N(10)	0.253(2)	0.392(2)	0.738(1)	16(2)	C(19)	0.472(2)	0.300(1)	0.633(1)	7(1)
C(1)	0.281(1)	0.4193(8)	0.3345(9)	3.2(7)	C(20)	0.203(6)	0.043(3)	0.594(3)	26(5)

[a] $B_{eq} = (8\pi^2/3)\sum_{i=1}^{3}\sum_{j=1}^{3}U_{ij}a_i^*a_j^*\bar{a}_i\bar{a}_j$.

Table V. Final Atomic Positional Parameters and B_{eq} Values (Å²) for $[Cu_4(M3)_2(\mu_3\text{-}OMe)_2(NCS)_4](DMF)$ (V)

atom	x	y	z	B_{eq}[a]	atom	x	y	z	B_{eq}[a]
Cu(1)	0.23429(3)	0.21767(4)	0.61794(8)	1.73(3)	C(4)	0.0128(3)	0.2460(4)	0.4210(7)	2.1(3)
Cu(2)	0.21424(4)	0.35095(4)	0.57602(8)	1.97(4)	C(5)	0.0486(3)	0.1989(4)	0.4710(7)	2.2(3)
S(1)	0.18131(8)	0.1555(1)	0.9168(2)	2.44(8)	C(6)	0.1035(3)	0.2082(4)	0.5173(6)	1.9(3)
S(2)	0.15012(8)	0.4310(1)	0.8316(2)	2.43(8)	C(7)	–0.0459(3)	0.2341(4)	0.3692(7)	2.9(3)
S(3)	0.39035(7)	0.1021(1)	0.8103(2)	2.13(7)	C(8)	0.1360(3)	0.1566(3)	0.5839(6)	1.8(3)
S(4)	0.3316(1)	0.5006(1)	0.5530(3)	4.6(1)	C(9)	0.2105(3)	0.1042(3)	0.7220(7)	2.2(3)
O(1)	0.1755(2)	0.2749(2)	0.5480(4)	1.8(2)	C(10)	0.2318(3)	0.1294(4)	0.8627(7)	2.5(3)
O(2)	0.2694(2)	0.2924(2)	0.6111(4)	2.0(2)	C(11)	0.1770(3)	0.2341(4)	0.8898(6)	2.1(3)
N(1)	0.1872(2)	0.1550(3)	0.6316(5)	1.9(2)	C(12)	0.1401(3)	0.2623(4)	0.9325(7)	2.5(3)
N(2)	0.2048(2)	0.2635(3)	0.8327(5)	1.9(2)	C(13)	0.1335(3)	0.3220(4)	0.9142(7)	2.6(3)
N(2)	0.1973(2)	0.3245(3)	0.8116(5)	1.9(2)	C(14)	0.1626(3)	0.3530(3)	0.8510(6)	1.9(3)
N(4)	0.1515(2)	0.3977(3)	0.5490(5)	1.9(2)	C(15)	0.1889(3)	0.4604(3)	0.7444(7)	2.5(3)
N(5)	0.2989(3)	0.1702(3)	0.6861(6)	2.5(3)	C(16)	0.1594(3)	0.4604(4)	0.5947(7)	2.5(3)
N(6)	0.2589(3)	0.4184(3)	0.5773(6)	2.9(3)	C(17)	0.1040(3)	0.3773(3)	0.5020(6)	2.0(3)
C(1)	0.1242(3)	0.2663(3)	0.5141(6)	1.5(3)	C(18)	0.3211(3)	0.3064(4)	0.7043(7)	2.4(3)
C(2)	0.0881(3)	0.3151(3)	0.4757(6)	1.7(3)	C(19)	0.3373(3)	0.1420(3)	0.7390(7)	1.8(3)
C(3)	0.0333(3)	0.3033(4)	0.4284(7)	2.2(3)	C(20)	0.2895(3)	0.4525(4)	0.5676(7)	2.5(3)

[a] $B_{eq} = (8\pi^2/3)\sum_{i=1}^{3}\sum_{j=1}^{3}U_{ij}a_i^*a_j^*\bar{a}_i\bar{a}_j$.

tetranuclear fragment is clearly defined. Pertinent crystallographic and other data for all compounds are given in Table I, and atomic coordinates are given in Tables II–VI (**I**, **III**–**V**, and **VII**, respectively). Hydrogen atom coordinates (Tables SI, SIII, SV, SVII, and SIX for **I**, **III**–**V**, and **VII**, respectively) and thermal parameters (Tables SII, SIV, SVI, SVIII, and SX for **I**, **III**–**V**, and **VII**, respectively) are included as supplementary material.

Results and Discussion

The condensation of 2,6-diformyl-4-methylphenol (DFP) with 3,6-bis((2-aminoethyl)thio)pyridazine (PTA) in the presence of copper(II) nitrate and trifluoromethanesulfonate (triflate), whose anions have significant coordinating ability, results in the formation of a 1:1 macrocyclic ligand (Figure 1, M3), which acts as a tridentate N_2O donor, with no significant involvement of the pyridazine nitrogen atoms. In contrast, if the same template condensation is carried out in the presence of $Cu(BF_4)_2$ or $Cu(ClO_4)_2$, involving essentially noncoordinating or very weakly coordinating anions, dinuclear complexes of the 34-membered, 2:2, macrocyclic ligands H_2M1 and H_2M2 (Figure 1) are produced,[36] in which the in-plane donor sets (N_4O_2) for the two

Table VI. Final Atomic Positional Parameters and B_{eq} Values (Å^2) for [Cu(M3)(NCS)$_2$] (VII)

atom	x	y	z	B_{eq}[a]	atom	x	y	z	B_{eq}[a]
Cu(1)	0.41690(3)	0.14748(6)	0.69368(3)	3.72(3)	C(8)	0.4069(3)	0.2350(5)	0.5620(3)	4.4(3)
Cu(2)	0.70004(3)	0.55644(6)	0.95677(3)	3.93(3)	C(9)	0.5062(4)	0.3045(6)	0.6573(3)	5.9(3)
S(1)	0.5712(1)	0.1256(2)	0.6173(1)	7.3(1)	C(10)	0.5684(3)	0.2191(6)	0.6835(3)	6.7(4)
S(2)	0.4136(1)	−0.3352(2)	0.6110(1)	7.8(1)	C(11)	0.5260(3)	−0.0042(6)	0.6185(3)	5.2(3)
S(3)	0.3656(1)	−0.1427(2)	0.8176(1)	9.0(1)	C(12)	0.5232(4)	−0.0930(7)	0.5729(4)	7.2(4)
S(4)	0.60083(8)	0.2319(2)	0.91262(8)	5.79(8)	C(13)	0.4887(4)	−0.1921(7)	0.5700(4)	6.7(4)
S(5)	0.60520(8)	0.7413(2)	0.77068(7)	4.98(7)	C(14)	0.4576(3)	−0.2019(5)	0.6149(3)	5.1(3)
S(6)	0.62004(8)	0.9757(1)	1.03480(8)	4.79(7)	C(15)	0.3763(5)	−0.3118(6)	0.6705(4)	9.0(5)
S(7)	0.83299(8)	0.6507(1)	1.19317(7)	4.84(7)	C(16)	0.3024(5)	−0.2633(8)	0.6361(4)	8.8(5)
S(8)	0.8967(1)	0.5090(3)	0.9170(2)	13.7(2)	C(17)	0.2794(3)	−0.1316(7)	0.5392(4)	6.5(4)
O(1)	0.3439(2)	0.0662(3)	0.6167(2)	3.9(2)	C(18)	0.3784(3)	−0.0342(5)	0.7771(3)	4.7(3)
O(2)	0.6277(2)	0.5723(3)	0.9863(2)	3.4(1)	C(19)	0.5382(3)	0.2197(4)	0.8345(3)	3.7(2)
N(1)	0.4957(2)	−0.0162(4)	0.6595(2)	4.4(2)	C(20)	0.5597(2)	0.5775(4)	0.9489(3)	3.0(2)
N(2)	0.4612(3)	−0.1175(4)	0.6577(2)	4.6(2)	C(21)	0.5179(2)	0.6313(4)	0.9771(2)	3.0(2)
N(3)	0.3000(3)	−0.1496(5)	0.6049(3)	6.0(3)	C(22)	0.4439(3)	0.6258(4)	0.9410(3)	3.6(2)
N(4)	0.4411(2)	0.2367(4)	0.6285(2)	3.9(2)	C(23)	0.4098(3)	0.5706(5)	0.8777(3)	3.7(2)
N(5)	0.3902(3)	0.0427(4)	0.7499(2)	5.2(2)	C(24)	0.4514(3)	0.5309(3)	0.8480(3)	3.8(2)
N(6)	0.4934(2)	0.2117(4)	0.7795(2)	5.0(2)	C(25)	0.5248(2)	0.5355(4)	0.8804(2)	3.2(2)
N(7)	0.6595(2)	0.7679(4)	0.9094(2)	3.6(2)	C(26)	0.3306(3)	0.5599(5)	0.8403(3)	5.2(3)
N(8)	0.6629(2)	0.8207(4)	0.9677(2)	3.6(2)	C(27)	0.5628(3)	0.5105(5)	0.8412(3)	3.9(2)
N(9)	0.6163(2)	0.7103(4)	1.0762(2)	3.4(2)	C(28)	0.6523(3)	0.5123(5)	0.8071(3)	4.7(3)
N(10)	0.6290(3)	0.5167(4)	0.8612(2)	3.7(2)	C(29)	0.6744(3)	0.6350(6)	0.7967(3)	4.8(3)
N(11)	0.7645(2)	0.5902(5)	1.0539(2)	5.0(2)	C(30)	0.6107(3)	0.8009(5)	0.8486(3)	3.7(2)
N(12)	0.7797(3)	0.5148(5)	0.9404(3)	6.6(3)	C(31)	0.5596(3)	0.8848(5)	0.8402(3)	4.6(3)
C(1)	0.3299(3)	0.0666(5)	0.5522(3)	3.9(2)	C(32)	0.5611(3)	0.9342(5)	0.8971(3)	4.5(3)
C(2)	0.2905(3)	−0.0288(6)	0.5096(3)	5.0(3)	C(33)	0.6165(3)	0.9011(4)	0.9615(3)	3.6(2)
C(3)	0.2693(3)	−0.0272(7)	0.4378(3)	6.7(4)	C(34)	0.6830(3)	0.8927(5)	1.1063(3)	4.1(2)
C(4)	0.2859(4)	0.0631(8)	0.4075(3)	6.6(4)	C(35)	0.6505(3)	0.7959(5)	1.1312(3)	4.1(2)
C(5)	0.3283(3)	0.1521(6)	0.4493(3)	5.6(3)	C(36)	0.5493(3)	0.6979(4)	1.0387(3)	3.5(2)
C(6)	0.3525(3)	0.1552(6)	0.5211(3)	4.1(3)	C(37)	0.7934(3)	0.6145(5)	1.1113(3)	3.9(2)
C(7)	0.2638(4)	0.0637(8)	0.3302(3)	10.1(5)	C(38)	0.8280(3)	0.5104(7)	0.9305(3)	6.8(4)

[a] $B_{eq} = (8\pi^2/3)\sum_{i=1}^{3}\sum_{j=1}^{3} U_{ij} a_i^* a_j^* \vec{a}_i \vec{a}_j$.

copper(II) ions are provided by the two phenolic fragments, which are twisted relative to each other by about 150°, with the PTA fragments forming straps across the dinuclear center. The high stability associated with the diphenoxide-bridged $Cu_2N_4O_2$ center is seen as the driving force for the formation of dinuclear derivatives, rather than the tetranuclear derivatives, which are considered as reasonable alternatives.

In the present study, it is clear that, because the anions present are reasonable ligands in their own right, there is no need to form a 2:2 macrocycle to satisfy the coordination requirements of the two copper(II) ions. Presumably, prior to addition of PTA, a dinuclear intermediate forms in which the two copper(II) ions are bonded to DFP, bridged by the phenoxide oxygen, and terminally bound by an anion. The increased electrophilic nature of the coordinated aldehydic carbonyl groups promotes attack by one end of a PTA molecule, which then, due to its flexibility, spans the dinuclear center in a "nonbonding" fashion.

The tetranuclear chloride, bromide, azide, and thiocyanate complexes were made metathetically from the nitrate, but the chloride complex (**III**) can be produced, in low yield, by the direct reaction of DFP and PTA with $CuCl_2$ in methanol. However, in this reaction, and also in the reaction involving $CuBr_2$, an unusual redox process occurs, producing mixed-oxidation-state, Cu(II)–Cu(I), species, as the major components.[45] That such a reaction does not occur in the synthesis of **III**–**VI** establishes the stability of **I** and its role as a suitable starting material for the metathetical synthesis of other complexes. The formation of a mononuclear copper thiocyanate complex as the major product in the template reaction involving copper(II) thiocyanate is somewhat unexpected, especially since the ligand remains neutral. The instability of copper(II) thiocyanate, and the precipitation of Cu^{I}SCN during the reaction, clearly changes the reaction stoichiometry but does not explain the obvious stability of the mononuclear species. However it is likely that the formation of the tetranuclear species (**V**) proceeds through the mononuclear compound, as an intermediate, since both compounds appear in the same reaction. The formation of **V** from **I** simply complements the other reactions.

The role of methanol and ethanol in these reactions, and in particular the formation of alkoxide-bridged complexes, rather than hydroxide-bridged species (water was not excluded and metal and other salts were not dried), is not clear. The highly basic nature of PTA itself may have assisted in deprotonating a coordinated alcohol molecule, thus forming a PTA salt. However no such species were detected.

Description of the Structures. (a) [Cu$_2$(M3)(μ_2-OMe)(NO$_3$)$_2$] (I). The structure of [Cu$_2$(M3)(μ_2-OMe)(NO$_3$)$_2$] (**I**) is shown in Figure 2, and bond lengths and bond angles relevant to the copper coordination spheres are given in Table VII. Each copper center has four short contacts to an azomethine nitrogen, bridging methoxide and phenoxide oxygens, and a nitrate oxygen, which form a roughly planar arrangement. The two copper centers are separated by 2.937(2) Å. The shortest Cu–O contacts are to the methoxide oxygen (Cu(I)–O(2) = 1.891(6) Å; Cu(2)–O(2) = 1.887(6) Å). The copper centers are displaced slightly from the mean plane of the NO_3 donor sets (Cu(1), −0.0915 Å; Cu(2), −0.0686 Å). A second oxygen atom on each coordinated nitrate lies within 2.60 Å of each copper center (Cu(1)–O(4) = 2.581(7) Å; Cu(2)–O(7) = 2.587(7) Å), suggesting the possibility of a weak "axial" interaction and that the nitrate groups should be considered as bidentate. The difference in Cu–O(nitrate) bond lengths of <0.6 Å has been previously regarded as an indication of significant bidentate coordination.[46] Two other distant contacts to pyridazine nitrogens N(2) and N(3) (Cu(1)–N(2) = 2.659(7) Å; Cu(2)–N(3) = 2.713(7) Å) should be considered insignificant, especially since the dihedral angle between the mean plane of the pyridazine ring and the N(1)–N(4)–Cu(1)–Cu(2)–O(3)–O(1)–O(2)–O(6) mean plane is 130.8°, indicating less than optimum orbital alignments. However the fact that the pyridazine is

(45) Tandon, S. S.; Thompson, L. K. Unpublished results.

(46) Addison, C. E.; Logan, N.; Wallwork, S. C.; Garner, C. D. *Q. Rev. Chem. Soc.* **1971**, *25*, 289.

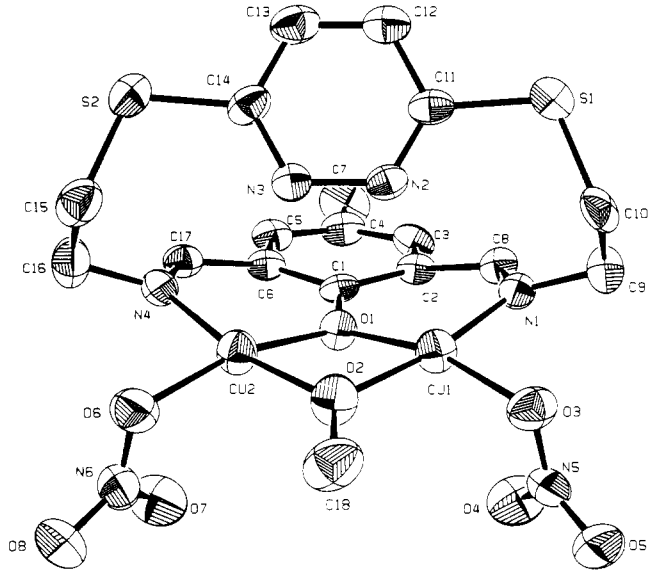

Figure 2. Structural representation of $[Cu_2(M3)(\mu_2\text{-}OMe)(NO_3)_2]$ (**I**) with hydrogen atoms omitted (50% probability thermal ellipsoids).

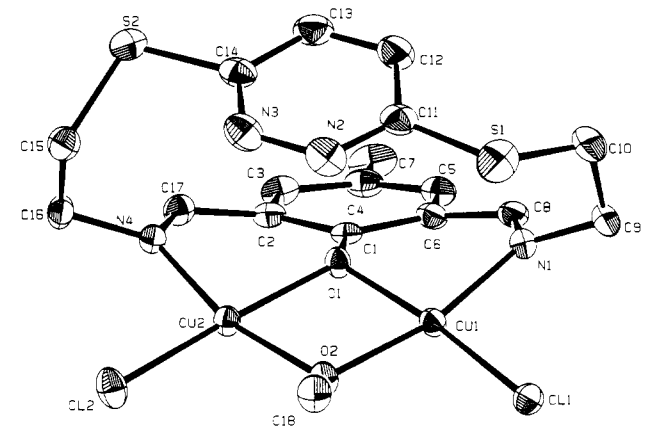

Figure 3. Structural representation of a dinuclear fragment of $[Cu_4(M3)_2(\mu_3\text{-}OMe)_2(\mu_2\text{-}Cl)_2Cl_2]$ (**III**) with hydrogen atoms omitted (50% probability thermal ellipsoids).

Table VII. Interatomic Distances (Å) and Angles (deg) Relevant to the Copper Coordination Spheres in $[Cu_2(M3)(\mu_2\text{-}OMe)(NO_3)_2]$ (**I**)

Cu(1)–O(1)	1.962(5)	Cu(2)–N(4)	1.952(7)
Cu(1)–O(2)	1.891(6)	Cu(1)–O(4)	2.581(7)
Cu(1)–O(3)	2.005(6)	Cu(1)–N(2)	2.659(7)
Cu(1)–N(1)	1.939(7)	Cu(2)–O(7)	2.587(7)
Cu(2)–O(1)	1.954(5)	Cu(2)–N(3)	2.713(7)
Cu(2)–O(2)	1.887(6)	Cu(1)–Cu(2)	2.937(2)
Cu(2)–O(6)	2.010(6)		
O(1)–Cu(1)–O(2)	78.6(2)	O(1)–Cu(1)–O(3)	165.2(2)
O(1)–Cu(1)–N(1)	91.7(2)	O(2)–Cu(1)–O(3)	92.9(2)
O(2)–Cu(1)–N(1)	169.4(3)	O(3)–Cu(1)–N(1)	97.5(3)
O(1)–Cu(2)–O(2)	78.9(2)	O(1)–Cu(2)–O(6)	165.5(2)
O(1)–Cu(2)–N(4)	91.9(3)	O(2)–Cu(2)–O(6)	94.1(2)
O(2)–Cu(2)–N(4)	168.3(3)	O(6)–Cu(2)–N(4)	96.4(3)
Cu(1)–O(1)–Cu(2)	97.2(2)	Cu(1)–O(2)–Cu(2)	102.1(2)

oriented with the nitrogen loan pairs pointing inward, toward the dinuclear center, raises the question as to whether these "pseudo-axial" contacts are in fact real. The fact that there is a slight tetrahedral distortion at each copper center, with O(1) and O(3) displaced by 0.105(6) and 0.121(6) Å, respectively, below and with O(2) and N(1) displaced by –0.157(7) and –0.138(7) Å, respectively, above the mean NO_3 "square plane" at Cu(1), with a similar situation at Cu(2), suggests that both axial-ligand effects are probably very weak and the copper ion coordination geometry should be regarded as predominantly square planar. The packing

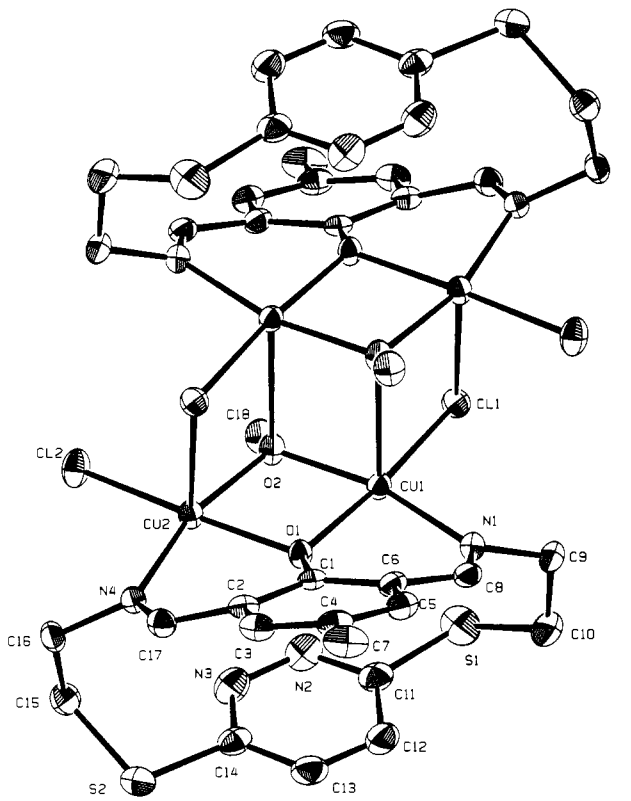

Figure 4. Structural representation of $[Cu_4(M3)_2(\mu_3\text{-}OMe)_2(\mu_2\text{-}Cl)_2Cl_2]$ (**III**) with hydrogen atoms omitted (50% probability thermal ellipsoids).

Table VIII. Interatomic Distances (Å) and Angles (deg) Relevant to the Copper Coordination Spheres in $[Cu_4(M3)_2(\mu_3\text{-}OMe)_2(\mu\text{-}Cl)_2Cl_2]$ (**III**)

Cu(1)–Cl(1)	2.262(1)	Cu(2)–N(2)	1.973(3)
Cu(1)–O(1)	1.978(3)	Cu(1)–Cu(2)	3.0667(9)
Cu(1)–O(2)	1.933(3)	Cu(1)–O(2)′	2.711(3)
Cu(1)–N(1)	1.982(3)	Cu(2)–Cl(1)	2.756(2)
Cu(2)–Cl(2)	2.250(1)	Cu(1)–Cu(1)′	3.387(2)
Cu(2)–O(1)	2.005(3)	Cu(1)–Cu(2)′	3.506(1)
Cu(2)–O(2)	1.941(3)		
Cl(1)–Cu(1)–O(2)	95.48(8)	Cl(2)–Cu(2)–O(2)	97.12(8)
Cl(1)–Cu(1)–N(1)	98.3(1)	Cl(2)–Cu(2)–N(2)	96.6(1)
O(1)–Cu(1)–O(2)	77.7(1)	O(1)–Cu(2)–O(2)	76.9(1)
O(1)–Cu(1)–N(1)	88.5(1)	O(1)–Cu(2)–N(2)	89.0(1)
O(2)–Cu(1)–N(1)	165.8(1)	O(2)–Cu(2)–N(2)	165.1(1)
Cl(2)–Cu(2)–O(1)	173.01(8)	Cu(1)–O(1)–Cu(2)	100.7(1)

diagram (Figure S1, supplementary material) indicates no intermolecular association.

(b) $[Cu_4(M3)_2(\mu_3\text{-}OMe)_2(\mu_2\text{-}Cl)_2Cl_2]$ (III). The structure of the dinuclear half of $[Cu_4(M3)_2(\mu_3\text{-}OMe)_2(\mu_2\text{-}Cl)_2Cl_2]$ (**III**) is shown in Figure 3, and bond lengths and bond angles relevant to the copper coordination spheres are given in Table VIII. Each dinuclear center in **III** consists of two pseudo-square-planar copper ions, separated by 3.0667(9) Å and bridged by phenoxide and methoxide oxygen atoms and bound terminally by azomethine nitrogens and chlorines. Cu–N and Cu–O distances compare closely with those in **I**. Cu(1) is displaced by 0.0244 Å from the O(1)–O(2)–N(1)–Cl(1) mean plane, while Cu(2) is displaced by 0.0769 Å from the O(1)–O(2)–N(4)–Cl(2) mean plane. The solid angle at O(1) is 351.2°, indicating an almost trigonal-planar phenoxide bridge, whereas at O(2) a solid angle of 343.2° indicates significant pyramidal distortion, quite different from the situation found in **I**. The orientation of the pyridazine ring in **III** is quite different from that in **I**, being almost parallel to the dinuclear center, with a dihedral angle of 0.66° between the pyridazine mean plane and the dinuclear Cu(1)–O(1)–O(2)–Cu(2) core. This clearly indicates no possible association between the pyridazine nitrogen donors and the copper atoms, in contrast to

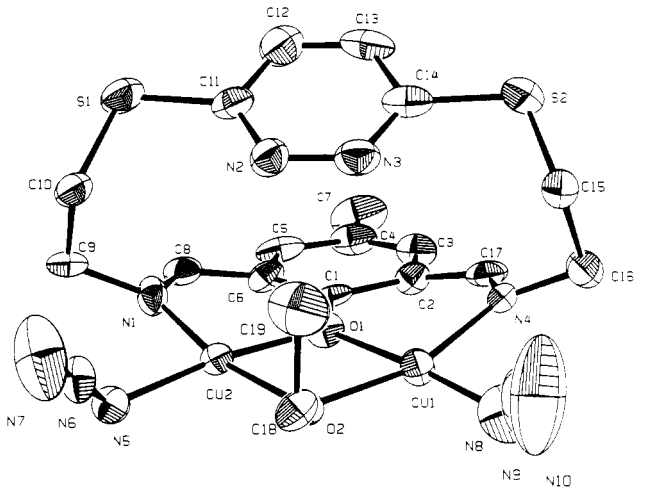

Figure 5. Structural representation of a dinuclear fragment of $[Cu_4(M3)_2(\mu_3\text{-}OEt)_2(\mu_2\text{-}N_3)_2(N_3)_2](MeOH)$ (**IV**) with hydrogen atoms omitted (50% probability thermal ellipsoids).

Table IX. Interatomic Distances (Å) and Angles (deg) Relevant to the Copper Coordination Spheres in $[Cu_4(M3)_2(\mu_3\text{-}OC_2H_5)_2(\mu_2\text{-}N_3)_2(N_3)_2](MeOH)$ (**IV**)

Cu(1)–O(1)	1.961(9)	Cu(2)–N(1)	1.93(1)
Cu(1)–O(2)	1.934(8)	Cu(2)–N(5)	1.96(1)
Cu(1)–N(4)	1.97(1)	Cu(1)–Cu(2)	3.039(3)
Cu(1)–N(8)	1.85(2)	Cu(1)–Cu(2)′	3.294(2)
Cu(2)–O(1)	1.955(8)	Cu(2)–Cu(2)′	3.279(3)
Cu(2)–O(2)	1.910(8)		
O(1)–Cu(1)–O(2)	76.2(3)	O(2)–Cu(2)–N(5)	95.9(4)
O(1)–Cu(1)–N(4)	90.5(4)	N(1)–Cu(2)–N(5)	95.4(5)
O(1)–Cu(1)–N(8)	175.6(6)	Cu(1)–O(1)–Cu(2)	101.8(4)
O(2)–Cu(1)–N(4)	162.7(4)	Cu(1)–O(2)–Cu(2)	104.5(4)
O(2)–Cu(1)–N(8)	100.9(6)	Cu(1)–O(3)–Cu(2)′	97.0(3)
N(4)–Cu(1)–N(8)	92.9(7)	Cu(2)–O(2)–Cu(2)′	97.0(3)
O(1)–Cu(2)–O(2)	76.9(3)	Cu(1)–N(5)–Cu(2)	95.5(4)
O(1)–Cu(2)–N(1)	92.1(4)	N(6)–N(5)–Cu(1)	133.8(9)
O(1)–Cu(2)–N(5)	171.8(4)	N(6)–N(5)–Cu(2)	127(1)
O(2)–Cu(2)–N(1)	167.5(4)		

the situation in **I**. The solid angle at O(2) is small enough to belie the presence of another bonding contact to O(2), and in fact the structure of **III** can best be represented as a dimer (Figure 4), in which the dinuclear halves are joined together by fairly long axial contacts (Cu(2)–Cl(1) = 2.756(2) Å; Cu(1)–O(2) = 2.711(3) Å), forming a tetranuclear core involving μ_3-methoxide and μ_2-chloride bridges and square-pyramidal copper centers. The tetranuclear core can be considered as a pair of cubes connected by a common Cu_2O_2 face, but with one vertex missing on each external face. Alkoxy groups, hydroxy groups, and even oxy groups have been shown in several cases to act as μ_3 bridges between copper centers, either to dimerize existing polynuclear entities[26,47-49] or to bridge a triangular arrangement of copper atoms.[50]

(c) $[Cu_4(M3)_2(\mu_3\text{-}OEt)_2(\mu_2\text{-}N_3)_2(N_3)_2](MeOH)$ (IV). The structure of a monomeric dinuclear fragment of **IV** is shown in Figure 5, and bond lengths and bond angles relevant to the copper coordination spheres are given in Table IX. The basic structural framework resembles that of each dinuclear half in **III**, with two essentially square-planar copper centers, separated by 3.039(3) Å and bridged by a phenoxide oxygen and an ethoxide oxygen and each bound terminally by an azide ligand. The short, in-plane Cu–N and Cu–O distances (Table IX) compare closely with those found in **I** and **III**. Cu(1) is displaced by 0.108(8) Å from the mean N(4)–N(8)–O(1)–O(2) plane and Cu(2) is displaced by 0.021(8) Å from the mean N(1)–N(5)–O(1)–O(2) plane. The solid angle at O(1) is 360.0°, indicating a completely trigonal-planar phenoxide bridge. Again the orientation of the pyridazine ring (dihedral angle of 25.0° from the Cu(1)–O(1)–O(2)–Cu(2) core) relative to the dinuclear center indicates no bonding between N(2) and N(3) and the copper atoms. Rather, as in the case of **III**, this provides an opportunity for two dinuclear halves to associate in a tetranuclear structure (Figure 6). As in **III**, the solid angle at the alkoxide bridge (346.2°) indicates dimeric association, and the two dinuclear units are bridged in an axial fashion, with relatively short contacts involving bridging μ_2(1,1)-azides (N(5)) and μ_3-ethoxides (Cu(1)–N(5) = 2.47(1) Å; Cu(2)–O(2)′ = 2.45(1) Å). The copper centers, therefore, have square-pyramidal structures as in **III**.

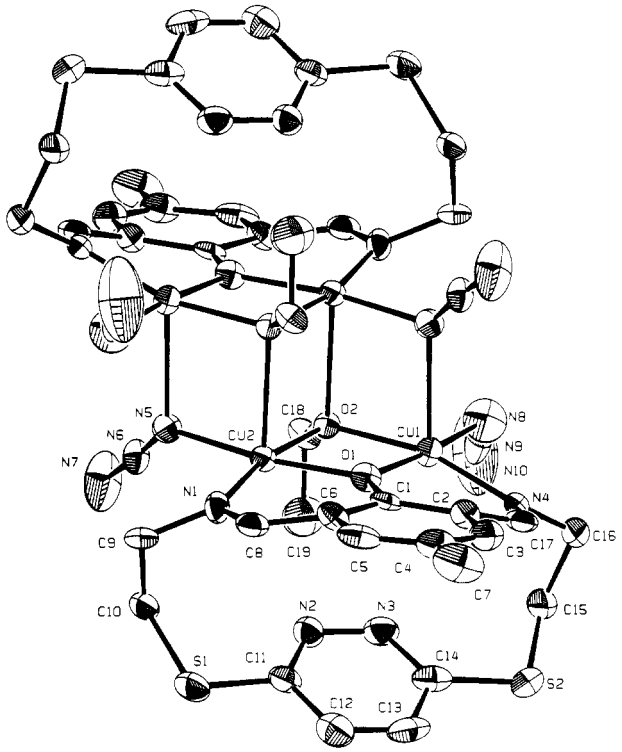

Figure 6. Structural representation of $[Cu_4(M3)_2(\mu_3\text{-}OEt)_2(\mu_2\text{-}N_3)_2(N_3)_2](MeOH)$ (**IV**) with hydrogen atoms omitted (50% probability thermal ellipsoids).

Structurally both **III** and **IV** are most unusual, in that they combine different axial bridges forming an open "box-kite" arrangement of two fused cubes, each missing one apex.

(d) $[Cu_4(M3)_2(\mu_3\text{-}OMe)_2(NCS)_4](DMF)$ (V). The basic dinuclear fragment in **V**, consisting of the familiar dinuclear copper(II) center, involving a μ_2-phenoxide bridge and a μ_2-methoxide bridge, is shown in Figure 7, and bond distances and angles relevant to the copper coordination spheres are given in Table X. In-plane copper–oxygen and copper–nitrogen distances, associated with the macrocyclic ligand and the methoxide bridge, compare closely with those in **I**, **III**, and **IV**. Copper–isothiocyanate distances (Cu(1)–N(5) = 1.951(6) Å; Cu(2)–N(6) = 1.927(8) Å) compare closely with those in the mononuclear derivative **VII**, and the two copper centers are separated by 3.009(1) Å. The N(5) terminal isothiocyanate group is essentially collinear with the copper–nitrogen bond (Cu(1)–N(5)–C(19) = 173.3(6)°), suggesting no additional bonding contacts from nitrogen N(5) to Cu(2) in the adjacent dimeric molecule. This appears to contradict the situation for some dimeric copper cyanate complexes where, despite almost linear Cu–NCO linkages (163.1, 164.8°), μ_2-cyanate angles less than 90° (83.5, 88.1°), and long coupling contacts (3.368, 2.620 Å), the dimeric associations are

(47) Barclay, G. A.; Hoskins, B. F. *J. Chem. Soc.* **1965**, 1979.
(48) Bertrand, J. A.; Kelly, J. A. *Inorg. Chim. Acta* **1970**, *4*, 203.
(49) Andrew, J. E.; Blake, A. B. *J. Chem. Soc., Dalton Trans.* **1973**, 1102.
(50) Cormarmond, J.; Dietrich, B.; Lehn, J.-M.; Louis, R. *J. Chem. Soc., Chem. Commun.* **1985**, 74.

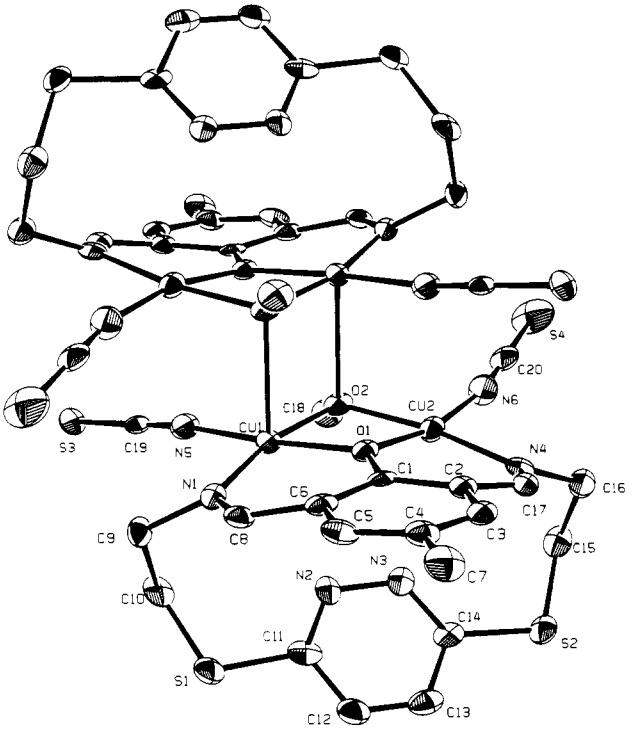

Figure 7. Structural representation of $[Cu_4(M3)_2(\mu_3\text{-}OMe)_2(NCS)_4](DMF)$ (V) with hydrogen atoms omitted (50% probability thermal ellipsoids).

Table X. Interatomic Distances (Å) and Angles (deg) Relevant to the Copper Coordination Spheres in $[Cu_4(M3)_2(\mu_3\text{-}OMe)_2(NCS)_4](DMF)$ (V)

Cu(1)–O(1)	1.965(5)	Cu(1)–O(2)	1.930(5)
Cu(1)–N(1)	1.938(6)	Cu(1)–N(5)	1.951(6)
Cu(2)–O(1)	1.953(5)	Cu(2)–O(2)	1.916(5)
Cu(2)–N(4)	1.930(6)	Cu(2)–N(6)	1.927(8)
Cu(1)–Cu(2)	3.009(1)	Cu(1)–O(2′	2.502(5)
Cu(1)–Cu(2)′	3.333(2)	Cu(2)–N(5)′	2.815(6)
Cu(1)–Cu(1)′	3.351(2)		
O(1)–Cu(1)–O(2)	77.1(2)	O(1)–Cu(1)–N(1)	91.4(2)
O(1)–Cu(1)–N(5)	172.0(2)	O(2)–Cu(1)–N(1)	166.6(2)
O(2)–Cu(1)–N(5)	95.0(2)	N(1)–Cu(1)–N(5)	96.6(3)
O(1)–Cu(2)–O(2)	77.7(2)	O(1)–Cu(2)–N(2)	92.4(2)
O(1)–Cu(2)–N(6)	167.3(2)	O(2)–Cu(2)–N(4)	169.1(2)
O(2)–Cu(2)–N(6)	94.3(3)	N(4)–Cu(2)–N(6)	96.2(3)
Cu(1)–O(1)–Cu(2)	100.3(2)	Cu(1)–O(2)–Cu(2)	103.0(2)

considered real.[51,52] The case for manganese and nickel isothiocyanate complexes appears to be more straightforward, where in typical examples much larger M–N(μ_2(1,1)-NCS)–M angles are observed (103.5,[53] 105.5° [54]), and the isothiocyanate group is symmetrically disposed between the metal centers. Unfortunately there appear to be no well-documented cases of genuine μ_2(1,1)-NCS-bridged dicopper(II) complexes. However symmetrical μ_2-isothiocyanate bridges would realistically be expected. The solid angle at the phenoxide oxygen O(1) is 358.9°, while the solid angle at the methoxide oxygen (344.0°) implies the presence of a dimeric contact. The interdimer Cu(1)–O(1) distances (2.502(5) Å) support this. The large Cu(2)–N(5) separation (2.815(6) Å) supports the earlier conclusion regarding the terminal nature of the thiocyanates (also supported by infrared studies), and so V is best described as a tetranuclear structure

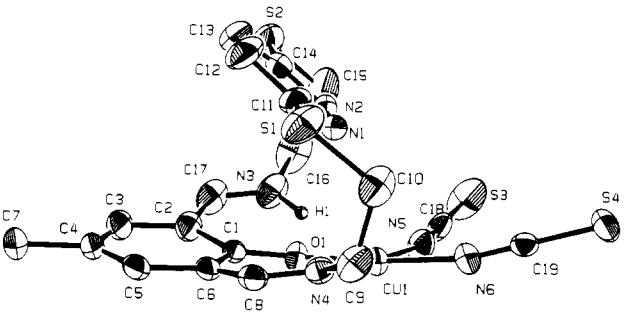

Figure 8. Structural representation of $[Cu(M3)(NCS)_2]$ (VII) with hydrogen atoms omitted (50% probability thermal ellipsoids).

Table XI. Interatomic Distances (Å) and Angles (deg) Relevant to the Copper Coordination Spheres in $[Cu(M3)(NCS)_2]$ (VII)

Cu(1)–O(1)	1.929(3)	Cu(2)–O(2)	1.923(3)
Cu(1)–N(4)	1.986(4)	Cu(2)–N(10)	1.991(4)
Cu(1)–N(5)	1.962(5)	Cu(2)–N(11)	1.966(5)
Cu(1)–N(6)	1.980(5)	Cu(2)–N(12)	1.941(5)
O(1)–Cu(1)–N(5)	84.4(2)	O(2)–Cu(2)–N(11)	84.4(2)
N(5)–Cu(1)–N(6)	89.2(2)	N(11)–Cu(2)–N(12)	89.9(2)
N(6)–Cu(1)–N(4)	96.5(2)	N(12)–Cu(2)–N(10)	94.1(2)
N(4)–Cu(1)–O(1)	89.7(2)	N(10)–Cu(2)–O(2)	91.2(2)
O(1)–Cu(1)–N(6)	172.6(2)	O(2)–Cu(2)–N(12)	168.4(2)
N(4)–Cu(1)–N(5)	172.8(2)	N(10)–Cu(2)–N(11)	175.0(2)

(Figure 7), with two square-pyramidal copper centers bridged axially via the methoxides and involving just terminally bound isothiocyanates. Cu(1) is displaced slightly from the mean plane of the four equatorial ligands (N(1)–N(5)–O(1)–O(2)) by 0.062(5) Å toward methoxide oxygen O(2) on the adjacent molecule, while the displacement of Cu(2) is 0.036(5) Å from the mean plane N(4)–N(6)–O(1)–O(2) away from the thiocyanate nitrogen in the adjacent dimeric molecule. While these displacements are small, they are consistent with the foregoing structural conclusions. The pyridazine mean plane has a dihedral angle of 42.0° with respect to the Cu_2O_2 mean plane, indicating no pyridazine nitrogen coordination.

(e) $[Cu(M3)(NCS)_2]$ (VII). The structure of **VII** reveals two chemically identical, but crystallographically independent, molecules in the asymmetric unit. Figure 8 depicts one of them, and bond distances and angles relevant to the copper coordination sphere are given in Table XI. The square-planar copper(II) center is coordinated in a cis arrangement with two bound isothiocyanates, an imine nitrogen (N(4)), and a phenolic oxygen (O(1)). The mean plane of the four donor atoms reveals no displacements greater than 0.0053(5) Å, and the copper center is displaced slightly from the mean plane (0.069 Å). A long contact from Cu(1) to pyridazine nitrogen N(1) (2.82 Å) might be considered as a possible bonding contact, but the dihedral angle of 45.03° between the mean pyridazine and CuN_3O planes clearly indicates that this is not the case. A similar situation exists with the other molecule. Another possible bonding contact exists between Cu(1) and S(7) on the neighboring molecule (Cu(1)–S(7) = 2.904(2) Å), supported by axial–equatorial angles close to 90°. This contact does not displace the copper significantly from the N_3O planar donor set and so is very weak. The Cu–O(phenol) distances are quite short (1.929(3) Å (Cu(1)); 1.923(3) Å (Cu(2))) and significantly shorter than similar distances in the other compounds. This is most unusual and suggests that the phenolic oxygen has lost its proton, behaving as a phenoxide anion. Since the complex is neutral, it is pertinent to locate the extra hydrogen, and fortunately it shows up in a difference map, attached to nitrogen N(3) (N(3)–H(1) = 0.99(6) Å) and N(9) (second molecule N(9)–H(2) = 0.84(4) Å). The sums of the angles around both N(3) and N(9) are 359 and 359.4°, respectively, indicating the trigonal-planar nature of these nitrogen atoms. The protonated nitrogens are hydrogen-bonded to the phenolic oxygens (O(1)–H(1) = 1.77(6) Å; O(2)–H(2) = 1.92(5) Å), indicating that the proton has

(51) Rojo, T.; Cortes, R.; Lezama, L.; Mesa, J. L.; Via, J.; Arriortua, M. I. *Inorg. Chim. Acta* **1989**, *165*, 91.
(52) Lloret, F.; Julve, M.; Faus, J.; Ruiz, R.; Castro, I.; Mollar, M.; Philoche-Levisalles, M. *Inorg. Chem.* **1992**, *31*, 784.
(53) Raghunathan, S.; Stevenson, C.; Nelson, J.; McKee, V. *J. Chem. Soc., Chem. Commun.* **1989**, 5.
(54) van Albada, G. A.; de Graff, R. A. G.; Reedijk, J. *Inorg. Chem.* **1984**, *23*, 1404.

Table XII. Spectroscopic and Magnetic Data

compound	λ_{max} (nm) (ϵ (L mol^{-1} cm^{-1}))	μ_{eff} (μ_B)	g	$-2J$ (cm^{-1})	ρ	10^6TIP (cgsu)	10^2R
$[Cu_2(M3)(\mu_2\text{-OMe})(NO_3)_2]$ (I) (Θ = 0 K)	670, 409[a] 693 (73), 388 (5900)[b]	1.02	2.06(1)	447(3)	0.006	59	1.1
$[Cu_2(M3)(\mu_2\text{-OMe})(CF_3SO_3)_2]\cdot 2C_2H_5OH$ (II) (Θ = 0 K)	671, 406[a] 694 (61), 407 (10 100)[b]	0.68	2.02(3)	632(7)	0.024	89	1.8
$[Cu_4(M3)_2(\mu_3\text{-OMe})_2(\mu_2\text{-Cl})_2Cl_2]$ (III) (Θ = 4 K)	786, 668, [445],[c] [395][a]	0.43	2.04(7)	822(16)	0.0025	37	1.5
$[Cu_4(M3)_2(\mu_3\text{-OEt})_2(\mu_2\text{-N}_3)_2(N_3)_2]$ (IV) (Θ = −31 K)	[836], 660, [620], 395[a]	0.58	2.00(4)	727(9)	0.0002	67	2.0
$[Cu_4(M3)_2(\mu_3\text{-OMe})_2(NCS)_4](DMF)$ (V) (Θ = 0 K)	[725], 607, 375[a]	0.71	2.14(6)	664(14)	0.001	83	1.74
$[Cu_4(M3)_2(\mu_3\text{-OMe})_2(\mu_2\text{-Br})_2Br]\cdot 2H_2O$ (VI) (Θ = 8 K)	[790], 636, 378[a]	0.38	2.09(9)	896(16)	0.006	40	0.86
$[Cu(N3)(NCS)_2]$ (VII)	666, 444[a]	1.86					

[a] Mull transmittance. [b] DMF solution. [c] [ ] = shoulder.

taken on the role of a Lewis acid in the absence of a copper ion. A comparison of the bond lengths in both of the C–N–C–C(phenyl) fragments reveals no really significant differences, even though N(3) would be considered to carry a formal charge.

Spectroscopy and Magnetism. The electronic spectra of complexes **I** and **II**, in the solid state, are characterized by single absorptions around 670 and 410 nm, associated with d–d and charge-transfer transitions, respectively (Table XII). These compounds have almost identical solid-state spectra, reflecting very similar copper ion coordination spheres and confirming the dinuclear structure for **II**. Although triflate is not renowned as a ligand, it is reasonable to assume that a triflate anion is coordinated to each copper ion to complete at least a square-planar array of ligands. In DMF a slight shift in the d–d band to lower energy in both cases suggests displacement of the coordinated anions by solvent molecules, and this is confirmed by conductance measurements (Λ_m(25 °C) = 118 (**I**) and 136 (**II**) mhos mol^{-1} cm^2), indicating the formation of 1:2 electrolytes. Complexes **III** and **IV** have more complex solid-state spectra, reflecting the different copper ion stereochemistries present in these tetranuclear complexes. Two prominent bands in the solid-state spectrum of the chloro complex (**III**) at 668 and 786 nm can reasonably be associated with Cu(1) ($CuNO_3Cl$) and Cu(2) ($CuNO_2Cl_2$), respectively. For the azido complex, two absorptions at 620 and 660 nm are reasonably assigned to Cu(1) with a square-pyramidal CuN_3O_2 chromophore, while the low-energy component at 836 nm is associated with Cu(2), a square-pyramidal CuN_2O_3 center. The bromo complex (**VI**) exhibits two prominent visible bands at 636 and 790 nm, which are very similar to those of the chloro complex and suggest the presence of two different copper(II) centers and a dimeric tetranuclear structure similar to that in **III**. The mononuclear isothiocyanate complex **VII** exhibits only one solid-state d–d band at 666 nm, associated with the single, square-planar copper(II) center, with a high-intensity charge-transfer band at 444 nm. The solid-state visible absorption spectrum of the tetranuclear isothiocyanate derivative (**V**) is different, with a strong, broad absorption at 600 nm and shoulders at 630 and 725 nm, which can be reasonably associated with both square-planar and square-pyramidal copper(II) centers, in keeping with the structural interpretation.

The coordinated 1:1 macrocyclic ligand M3 has a characteristic, strong CN stretching frequency in all the complexes in a very narrow range (1628–1637 cm^{-1}) in the infrared, which contrasts sharply with a comparable absorption for dinuclear copper complexes of the analogous 2:2 macrocyclic ligands, which fall in the range 1623–1625 cm^{-1}.[36] The role of coordinated nitrate can be assessed by infrared spectroscopy, in a region of the spectrum where combination ($\nu_1 + \nu_4$) bands occur for coordinated nitrate.[55] Three prominent bands are observed for **I** at 1714, 1719, and 1744 cm^{-1}, with a shoulder at 1740 cm^{-1}, associated with nitrate combination modes. The four bands are clearly associated with two different nitrates, and the separations of 25 cm^{-1} (1744 − 1719 cm^{-1}) and 26 cm^{-1} (1740 − 1714 cm^{-1}) are relatively small, suggesting the presence of monodentate nitrates, thus supporting the structural data. The azide complex **IV** exhibits three prominent azide bands at 2078, 2064, and 2035 cm^{-1}. Absorptions in this region are typical of species with both terminal and 1,1-bridging azides and compare closely with asymmetric azide stretching bands in both $[PPh_4]_2[Cu_2(N_3)_6]$[56] and $\{[Cu_2(H_2\text{-}L2)][Cu_2(N_3)_6]\}_n$.[57] Complex **V** exhibits one strong, sharp band at 2077 cm^{-1}, associated with terminally bound isothiocyanate, consistent with the structural interpretation, which excludes possible isothiocyanate bridging between the dinuclear halves. The mononuclear isothiocyanate complex (**VII**) has a much more complicated spectrum in the CN stretching region, with three discernible bands at 2109, 2082 (shoulder), and 2072 cm^{-1}. These absorptions are consistent with a cis arrangement of isothiocyanates, and the observation of three bands is consistent with the presence of two slightly different copper centers in the structure. The infrared spectrum of **VI** is very similar to that of **III**, supporting the suggested tetranuclear structure involving μ_3-methoxide and μ_2-bromide bridges.

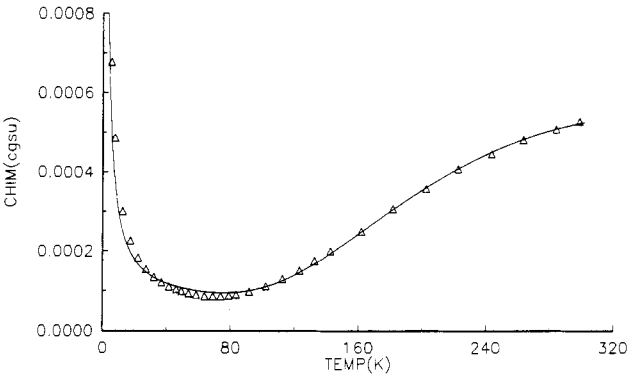

Figure 9. Magnetic data for $[Cu_2(M3)(\mu_2\text{-OMe})(NO_3)_2]$ (**I**). The solid line was calculated from eq 1 with g = 2.06(1), $-2J$ = 447(3) cm^{-1}, ρ = 0.006, and $N\alpha$ = 59 × 10^{-6} cgsu (10^2R = 1.1).

Compounds **I** and **II** have low room-temperature magnetic moments (Table XII), typical of antiferromagnetically coupled dinuclear copper(II) complexes. Variable-temperature magnetic data have been obtained for **I** and **II** in the temperature range 4–300 K, and the experimental susceptibility data for **I** are shown in Figure 9. Increasing susceptibility with increasing temperature, with a maximum above room temperature, typifies an antiferromagnetically coupled system. The steep rise in susceptibility at low temperature indicates the presence of a small amount of paramagnetic impurity. The data were fitted to the Bleaney–Bowers expression (eq 1)[58] using the isotropic (Heisenberg) exchange Hamiltonian ($H = -2Js_1s_2$) for two interacting $S = {}^1/_2$ centers (χ_m is expressed per mole of copper atoms, $N\alpha$ is the temperature-independent paramagnetism, ρ is the fraction of

(55) Lever, A. B. P.; Mantovani, E.; Ramaswamy, B. S. *Can. J. Chem.* **1971**, *49*, 1957.

(56) Fenske, D.; Steiner, K.; Dehnicke, K. *Z. Anorg. Allg. Chem.* **1987**, *553*, 57.

(57) Tandon, S. S.; Thompson, L. K.; Bridson, J. N.; McKee, V.; Downard, A. J. *Inorg. Chem.* **1992**, *31*, 4635.

(58) Bleaney, B.; Bowers, K. D. *Proc. R. Soc. London, A* **1952**, *214*, 451.

$$\chi_m = \frac{N\beta^2 g^2}{3k(T-\Theta)}[1 + {}^1/_3 \exp(-2J/kT)]^{-1}(1-\rho) + \frac{(N\beta^2 g^2)\rho}{4kT} + N\alpha \quad (1)$$

monomeric impurity, and Θ is a corrective, Weiss-like term to account for possible interdimer magnetic associations[59,60]).

A nonlinear regression analysis of the data was carried out with ρ as a floating parameter. The best fit line is shown in Figure 9 (solid line) for $g = 2.058(14)$, $-2J = 447(3)$ cm^{-1}, $\rho = 0.0060$, $N\alpha = 59 \times 10^{-6}$ cgsu, and $\Theta = 0$ K ($10^2R = 1.1$; $R = [\Sigma(\chi_{obs} - \chi_{calc})^2/\Sigma(\chi_{obs})^2]^{1/2}$). A similar analysis of variable-temperature data for **II** showed much stronger antiferromagnetic exchange with $-2J = 632(7)$ cm^{-1} (Table XII; $\Theta = 0$ K).

Antiferromagnetic exchange in **I** occurs, via a superexchange mechanism, through the two oxygen bridges (O(1), O(2)). While a study of the magnetostructural relationships for a series of dihydroxy-bridged copper(II) complexes involving a planar Cu_2O_2 ring, and d_{xy} ground state, reveals a linear relationship between exchange and hydroxide bridge angle,[61] no definitive studies for either dialkoxy- ($Cu_2(OR)_2$-) or diphenoxy-bridged species have been carried out. For derivatives involving essentially planar $[CuX(OCH_2CH_2NR_2)]_2$ (R = Me, Et, nPr; X = Cl, Br, NCO) arrays, a roughly linear relationship was demonstrated between $2J$ and Cu–O–Cu angle (96–105°).[62] For diphenoxy-bridged macrocyclic dicopper(II) complexes, involving in-plane $Cu_2O_2N_4$ donor sets, derived by template condensation of isophthalaldehydes with a variety of diamine linkages, a similar, roughly linear relationship between exchange integral ($-2J$) and Cu–O–Cu angle (99–104°) has been demonstrated.[63] On the basis of these "linear" relationships, an average value for $-2J$ for an alkoxide bridge angle of 102.1° and a phenoxide bridge angle of 97.2° is of the order of 500 cm^{-1}, which agrees reasonably well with the observed value for **I**. The substantially larger $-2J$ value for **II** is an indication of a larger average Cu–O(R)–Cu angle at the dinuclear center. No corrective terms for interdimer association were necessary in the data fitting of these compounds, in keeping with the structural interpretation.

Room-temperature magnetic moments for **III**–**VI** (Table XII) fall in the range 0.38–0.71 μ_B, indicating very strong antiferromagnetic coupling between the copper(II) centers. The dimeric association in the chloro complex (**III**) is considered to be weak because of the long interdimer contacts involving the methoxide and chloride bridges. As a consequence, any magnetic interactions between the dimer halves might be expected to be weak also. Variable-temperature magnetic data for **III** were fitted to eq 1, with the inclusion of a Θ term. After many regression analyses, the best data fit gave $-2J = 822(16)$ cm^{-1} and $\Theta = 4$ K (Table XII), and it was clear that the interdimer associative term was real, but very small. Such a small positive value indicates a very weak ferromagnetic interaction between the dimer halves in the tetranuclear structure, which is consistent with the nominally orthogonal nature of the axial interactions between the dinuclear halves in **III**. In other examples involving similar dimerizations, with weak axial interactions between copper(II) centers and alkoxide bridges,[49,64] the Bleaney–Bowers equation was considered adequate and any axial coupling was considered to be very weak also.

The complex (acetylacetonato)(*o*-hydroxyanilato)copper(II)[47] has a dinuclear phenoxide bridged structure, which actually involves axial dimeric association via the phenoxide oxygens (Cu–O = 2.64 Å) to produce a tetranuclear species comparable to **III**–**V**. A related complex, (acetylacetonato)(2-hydroxy-5-nitroanilato)copper(II),[65] which was suggested to have a similar tetranuclear structure involving axial μ_3-phenoxide bridges, was studied by variable-temperature magnetism by Hatfield in the range 100–400 K.[65] The susceptibility data were fitted to a tetranuclear model (rhombus) based on three exchange integrals. Local, equatorial, intradimer exchange via the phenoxide bridges was found to be antiferromagnetic ($J = -140$ cm^{-1}) as might be expected, while interdimer exchange was found to comprise two terms, one ferromagnetic ($J = +134$ cm^{-1}) and the other, involving the direct axial contacts, surprisingly antiferromagnetic and not trivial ($J = -48$ cm^{-1}). Further examination of this complex by Sinn[66] effectively rejects the tetranuclear model, largely on the basis of the magnitude and sign of the axial interaction, and suggests that a dimer treatment, with a paramagnetic impurity correction, adequately describes the coupling situation. It is interesting to note that data treatment by both models gave very high g values (>2.3).

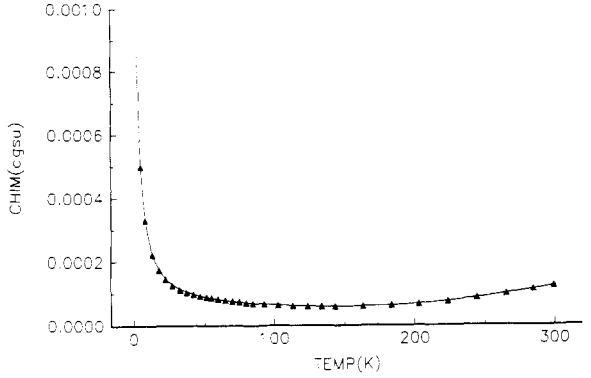

Figure 10. Magnetic data for $[Cu_4(M3)_2(\mu_3\text{-}OMe)_2(\mu_2\text{-}Br)_2Br_2]\cdot 2H_2O$ (**VI**). The solid line was calculated from eq 1 with $g = 2.09(9)$, $-2J = 896(16)$ cm^{-1}, $\rho = 0.006$, $N\alpha = 40 \times 10^{-6}$ cgsu, and $\Theta = 8$ K ($10^2R = 0.86$).

The bromo complex (**VI**) behaves similarly to **III**, and reasonable regressions are only possible with a nonzero Θ term. This complex exhibits the strongest intradimer antiferromagnetic exchange ($-2J = 896(16)$ cm^{-1}), with a slightly larger interdimer term (8 K), indicating again significant but small interdimer ferromagnetic coupling. Figure 10 illustrates the experimental data and the best fit theoretical line. That data for such strongly coupled systems, with such low room-temperature magnetic moments, can be successfully fitted to eq 1 strongly supports the validity of the measurements and the structural comparison between **III** and **VI**. A similar analysis of the data for the tetranuclear isothiocyanate complex (**V**) reveals moderately strong intradimer antiferromagnetic exchange and no interdimer coupling. This is consistent with the somewhat larger distance of separation between the dimer halves compared with that in **III** and the terminal nature of the thiocyanates.

The azide complex tells a different story, with a less than satisfactory fit of the data to the modified Bleaney–Bowers equation. The most reasonable fit of the data to eq 1 indicates strong intradimer antiferromagnetic coupling ($-2J = 727(9)$ cm^{-1}; $10^2R = 2.0$), which is consistent with the local Cu_2O_2 exchange framework but with a fairly large, negative Θ value (−30.6 K). This is not a good data fit, in particular in the low-temperature region below 100 K, and suggests either that the data are questionable or that eq 1 is inappropriate. Assuming the Θ value to be real, it suggests that coupling between the dimer halves is much stronger in this case and that it is antiferromagnetic in

(59) Watkins, N. T.; Dixon, E. A.; Crawford, V. H.; McGregor, K. T.; Hatfield, W. E. *J. Chem. Soc., Chem. Commun.* **1973**, 133.
(60) Sikorav, S.; Bkouche-Waksman, I.; Kahn, O. *Inorg. Chem.* **1984**, *23*, 490.
(61) Crawford, V. H.; Richardson, H. W.; Wasson, J. R.; Hodgson, D. J.; Hatfield, W. E. *Inorg. Chem.* **1976**, *15*, 2107.
(62) Merz, L.; Haase, W. *J. Chem. Soc., Dalton Trans.* **1980**, 875.
(63) Thompson, L. K. Unpublished results.
(64) Barraclough, C. G.; Brookes, R. W.; Martin, R. L. *Aust. J. Chem.* **1974**, *27*, 1843.
(65) Hatfield, W. E.; Inman, G. W. *Inorg. Chem.* **1969**, *8*, 1376.
(66) Sinn, E. *Inorg. Chem.* **1970**, *10*, 2376.
(67) Kahn, O. *Inorg. Chim. Acta* **1982**, *62*, 3.

nature and consistent with Hatfield's earlier observations. The interdimer contacts are significantly shorter in **IV** than in the other compounds (Cu(2)–O(2)′ = 2.443(8) Å; Cu(1)–N(5)′ = 2.47(1) Å), and the suggested axial antiferromagnetic coupling could be ascribed to a combination of axial azide and ethoxy interactions. At this time, we have not considered a tetranuclear model to describe these complexes. However, considering the facts that, for compounds **III**, **V**, and **VI**, Θ values are small, implying little interdimer interaction, and that $-2J$ values are very large anyway, the fitting of the susceptibility data to an expression with four possible J values is highly questionable and is not likely to result in an improved data fit. The exercise may be worthwhile for the azide complex and will be attempted as part of a future study.

Acknowledgment. We thank the Natural Sciences and Engineering Research Council of Canada for financial support of this study.

Supplementary Material Available: Tables of hydrogen atom coordinates (Tables SI, SIII, SV, SVII, and SIX), anisotropic thermal parameters (Tables SII, SIV, SVI, SVIII, and SX), bond distances and angles (Tables SXI–SXV), and least-squares planes (Tables SXVI–SXX) for **I**, **III**–**V**, and **VII**, respectively, and a packing diagram for **I** (Figure S1) (58 pages). Ordering information is given on any current masthead page.